

ORIGINAL RESEARCH

UCP3 (Uncoupling Protein 3) Insufficiency Exacerbates Left Ventricular Diastolic Dysfunction During Angiotensin II-Induced Hypertension

Xu Chen, PhD; Sadia Ashraf , PhD; Nadia Ashraf , MD; Romain Harmancey , PhD

BACKGROUND: Left ventricular diastolic dysfunction, an early stage in the pathogenesis of heart failure with preserved ejection fraction, is exacerbated by joint exposure to hypertension and obesity; however, the molecular mechanisms involved remain uncertain. The mitochondrial UCP3 (uncoupling protein 3) is downregulated in the heart with obesity. Here, we used a rat model of UCP3 haploinsufficiency (*ucp3^{+/-}*) to test the hypothesis that decreased UCP3 promotes left ventricular diastolic dysfunction during hypertension.

METHODS AND RESULTS: *Ucp3^{+/-}* rats and *ucp3^{+/+}* littermates fed a high-salt diet (HS; 2% NaCl) and treated with angiotensin II (190 ng/kg per min for 28 days) experienced a similar rise in blood pressure (158±4 versus 155±7 mm Hg). However, UCP3 insufficiency worsened diastolic dysfunction according to echocardiographic assessment of left ventricular filling pressures (E/e' ; 18.8±1.0 versus 14.9±0.6; $P<0.05$) and the isovolumic relaxation time (24.7±0.6 versus 21.3±0.5 ms; $P<0.05$), as well as invasive monitoring of the diastolic time constant (τ ; 15.5±0.8 versus 12.7±0.2 ms; $P<0.05$). Exercise tolerance on a treadmill also decreased for HS/angiotensin II-treated *ucp3^{+/-}* rats. Histological and molecular analyses further revealed that UCP3 insufficiency accelerated left ventricular concentric remodeling, detrimental interstitial matrix remodeling, and fetal gene reprogramming during hypertension. Moreover, UCP3 insufficiency increased oxidative stress and led to greater impairment of protein kinase G signaling.

CONCLUSIONS: Our findings identified UCP3 insufficiency as a cause for increased incidence of left ventricular diastolic dysfunction during hypertension. The results add further support to the use of antioxidants targeting mitochondrial reactive oxygen species as an adjuvant therapy for preventing heart failure with preserved ejection fraction in individuals with obesity.

Key Words: diastolic function ■ hypertension ■ obesity ■ oxidative stress ■ uncoupling protein

Heat failure with preserved ejection fraction (HFpEF) accounts for more than half of all heart failure cases and bears unacceptably high 5-year hospital readmission and mortality rates.¹ Left ventricular diastolic dysfunction (LVDD) is an early but underinvestigated stage in the pathogenesis of HFpEF.² Along with hypertension, obesity and obesity-related metabolic disorders represent major preventable causes for LVDD.^{3,4} Thus the prevalence of LVDD ranges between 20% to 30% in the general adult population but can go

as high as 65% in elderly individuals with hypertension, obesity, and diabetes.² Although there is some clinical evidence to support a role for an interaction between hypertension and obesity-related metabolic derangements in the exacerbation of LVDD,^{5,6} the nature of the molecular mechanisms at play remains uncertain.

UCP3 (uncoupling protein 3) is a mitochondrial anion carrier protein predominantly expressed in brown adipose tissue, skeletal muscle, and the heart.⁷ While the physiological functions of the protein have not been

Correspondence to: Romain Harmancey, PhD, Department of Physiology and Biophysics, University of Mississippi Medical Center, 2500 N. State St., Jackson, MS 39216-4505. E-mail: rharman@umc.edu

For Sources of Funding and Disclosures, see page 14.

© 2021 The Authors. Published on behalf of the American Heart Association, Inc., by Wiley. This is an open access article under the terms of the Creative Commons Attribution-NonCommercial-NoDerivs License, which permits use and distribution in any medium, provided the original work is properly cited, the use is non-commercial and no modifications or adaptations are made.

JAHA is available at: www.ahajournals.org/journal/jaha

CLINICAL PERSPECTIVE

What Is New?

- UCP3 (uncoupling protein 3) insufficiency exacerbates development of left ventricular diastolic dysfunction during hypertension.
- The dysfunction is linked to increased left ventricular wall thickening, detrimental molecular remodeling of the extracellular matrix and cardiomyocytes, and impairment of protein kinase G signaling.
- All those alterations can be traced back to a worsening of myocardial oxidative stress.

What Are the Clinical Implications?

- The results may help explain how obesity and type 2 diabetes lead to a greater incidence of left ventricular diastolic dysfunction in individuals with hypertension.
- The findings add further support to the use of antioxidants targeting mitochondrial oxidative stress as an adjuvant therapy for preventing heart failure with preserved ejection fraction in individuals with obesity.

Nonstandard Abbreviations and Acronyms

ECM	extracellular matrix
HFpEF	heart failure with preserved ejection fraction
HS/Ang II	high dietary salt intake combined with angiotensin II infusion
LVDD	left ventricular diastolic dysfunction

clearly delineated, muscle mitochondria lacking UCP3 have been shown to generate more superoxide anions under stimulated respiration.⁸ Hearts from UCP3 knockout mice also generate more reactive oxygen species (ROS) in response to ischemia/reperfusion, leading to further deterioration of contractile function following myocardial infarction.⁹ Using a rat model of UCP3 haploinsufficiency (*ucp3*^{+/-}) we demonstrated that, similar to the knockout experiments, partial loss of UCP3 is associated with a greater generation of mitochondrial ROS in cardiomyocytes and the exacerbation of left ventricular contractile dysfunction at reperfusion following ischemia.¹⁰ All together, these observations support the notion that UCP3 deficiency exacerbates myocardial cell injury in pathological conditions associated with enhanced mitochondrial ROS production.^{7,10}

Oxidative stress plays a key role in the development of diastolic dysfunction and the pathogenesis

of HFpEF.¹¹ Obesity-induced hypertension is characterized by activation of the sympathetic nervous and renin-angiotensin-aldosterone systems. On the one hand, increased myocardial energy demand driven by the increases in workload and β -adrenergic receptor activation stimulates mitochondrial ROS production.¹² On the other hand, angiotensin II (Ang II) directly signals through the Ang II receptor type 1 to increase ROS generation from both nicotinamide adenine dinucleotide phosphate (NADPH) oxidases and mitochondrial sources.¹³ We and others have previously reported that UCP3 is down-regulated with obesity and type 2 diabetes.^{10,14,15} Therefore, we propose that UCP3 insufficiency is 1 of the mechanisms linking obesity to accelerated development of LVDD during hypertension through exacerbation of myocardial oxidative stress.

To test our hypothesis, non-obese and metabolically normal male *ucp3*^{+/-} rats were subjected to chronic elevation in blood pressure by slow-pressor angiotensin II infusion under high dietary salt intake (HS/Ang II), a well-established method for induction of neurogenic hypertension.¹⁶ Cardiac function was evaluated with transthoracic echocardiography and invasive left ventricular (LV) pressure measurements. Mechanistic causes for LV dysfunction were further sought by histology and through targeted analyses of cardiac primary transcripts and proteins.

METHODS

The data that support the findings of this study are available from the corresponding author upon reasonable request.

Animals and Diets

Generation of the Sprague Dawley rat model of UCP3 haploinsufficiency has been reported previously.¹⁰ Because lack of UCP3 has no impact on adiposity or insulin sensitivity in rats maintained under conventional housing conditions,¹⁷ the model allowed testing of the present hypothesis independently from the confounding effects of obesity and diabetes. Male UCP3 insufficient rats (*ucp3*^{+/-}) and wild-type controls (*ucp3*^{+/+}) were obtained from same litters by non-brother-sister mating of heterozygous knockout rats. Animals were housed in the animal facilities of the Center for Comparative Research from the University of Mississippi Medical Center on a 12-hours light/12-hours dark cycle at a temperature of 22 °C \pm 2 °C and 40%–60% humidity. Rats (*n*=45 *ucp3*^{+/-} and 39 *ucp3*^{+/+}) were fed a non-purified standard laboratory rodent diet (22/5 rodent diet no. 8640; 0.4% NaCl; Teklad, Madison, WI) until 8 weeks of age, after which approximately half of the rats (*n*=24 *ucp3*^{+/-} and 24 *ucp3*^{+/+}) were randomly

selected to be fed a high-salt purified diet (D17030; 2% NaCl; Research Diets, New Brunswick, NJ) while the other half ($n=21$ $ucp3^{+/-}$ and 15 $ucp3^{+/+}$) were fed a matched low salt control diet (D17019; 0.4% NaCl; Research Diets). Drinking water was supplied ad libitum until end of the study protocol (Figure 1). The study complied with the Guide for the Care and Use of Laboratory Animals and was approved by the Institutional Animal Care and Use Committee (protocol #1436A). All efforts were made to minimize animal suffering and to reduce the number of animals used. Four rats in the HS/Ang II treatment groups (2 $ucp3^{+/+}$ rats and 2 $ucp3^{+/-}$ rats) died before the end of the protocol and the partial data on these animals were not included in the analyses.

Ang II Treatment

After 2 weeks on purified diets, 0.9% saline or Ang II (Bachem, Torrance, CA) was administered at a rate of 190 ng/kg per minute (nominal infusion rate: 2.42 μ L/h) for 28 days via Alzet osmotic pump implanted subcutaneously (model 2ML4; DURECT Corporation, Cupertino, CA). Animals were anesthetized with isoflurane (2.5% isoflurane in 100% O₂) and injected subcutaneously with buprenorphine sustained-release (1 mg/kg) before pump implantation.

Blood Pressure and Heart Rate Measurements

Mean arterial blood pressure and heart rate were measured in conscious rats using the CODA non-invasive blood pressure system (Kent Scientific, Torrington, CT). Animals were subjected to tail-cuff measurements for 5 consecutive days for baseline values before osmotic pump implantation, and then for 2 consecutive days every week following initiation of Ang II or 0.9% saline treatment. Mean values of blood pressure and heart rate were calculated for each time point and used for statistical analyses.

Transthoracic Echocardiography

Echocardiographic exams were performed under isoflurane anesthesia using a Vevo 3100 Imaging System (FUJIFILM VisualSonics, Toronto, Ont). The amount of isoflurane dispensed (1%–2% isoflurane in 100% O₂) was individually adjusted to maintain similar heart rate between rats. Body temperature was maintained within physiological range (36.0 °C–37.5 °C) throughout the procedure using a dedicated heating pad. B-Mode and M-Mode images were obtained from the parasternal long-axis view and used to calculate aortic root diameter, left ventricular anterior wall thickness at end-diastole, LV internal diameter at end-diastole,

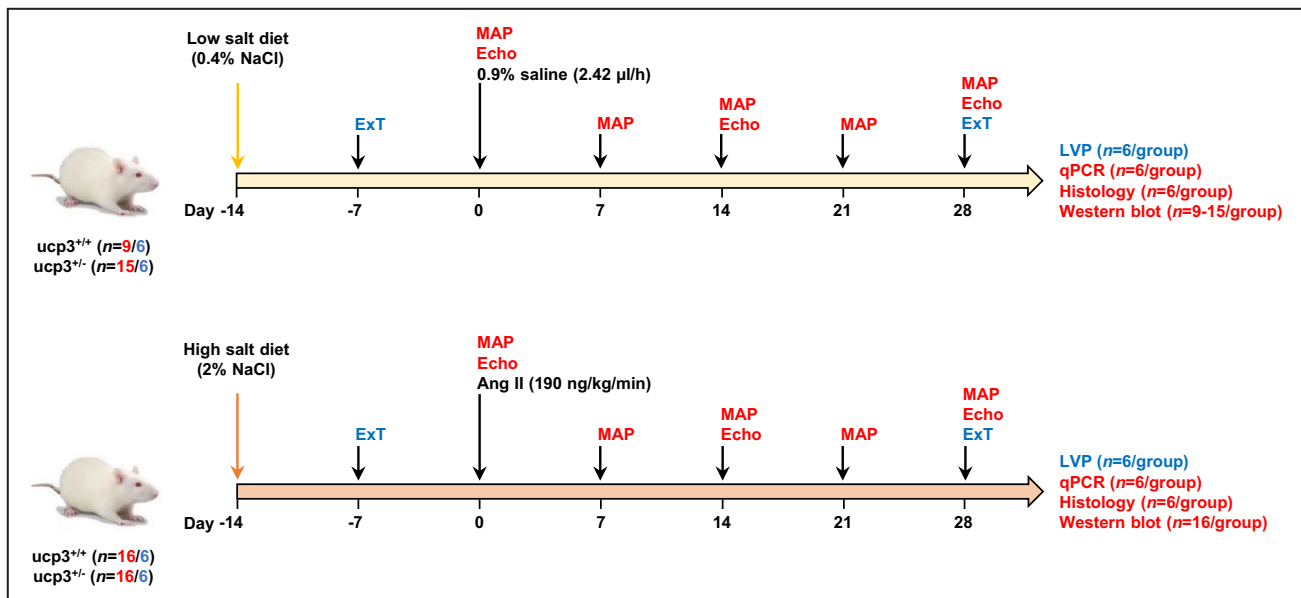


Figure 1. Study protocol used to determine the impact of UCP3 (uncoupling protein 3) insufficiency on cardiac structural and functional remodeling during hypertension.

A first cohort of $ucp3^{+/-}$ and $ucp3^{+/+}$ rats (red; $n=9$ –16 per group) was used to assess in vivo the evolution of the mean arterial blood pressure (weekly measurements) as well as cardiac structure and function (transthoracic echocardiography; bi-weekly measurements) over the course of a combination treatment consisting in high dietary salt intake (2% NaCl) and chronic Ang II infusion (190 ng/kg per min; Bottom panel). Control animals were maintained on a low-salt diet and infused with 0.9% saline (Top panel). Cardiac tissue was collected after euthanasia for further molecular analyses. The protocol was repeated on a second cohort of $ucp3^{+/-}$ and $ucp3^{+/+}$ rats (blue; $n=6$ per group) to determine the impact of the treatment on exercise tolerance on a treadmill and left ventricular pressure. Numbers only include rats that completed the experimental protocol. Ang II indicates angiotensin II; ExT, exercise tolerance on a treadmill; MAP, mean arterial pressure; qPCR, quantitative polymerase chain reaction; and UCP3, uncoupling protein 3.

LV posterior wall thickness at end-diastole, corrected LV mass, LV ejection fraction, and LV fractional shortening. Peak velocity blood flow from LV relaxation in early diastole (E wave), early diastolic mitral annular velocity (e'), isovolumic relaxation time, isovolumic contraction time, left ventricular ejection time, and LV myocardial performance index ([isovolumic relaxation time+isovolumic contraction time]/left ventricular ejection time) were derived from Doppler analyses performed in the apical 4-chamber view.

Exercise Tolerance Test

Maximal tolerance to exercise was determined on a Exer-6 animal treadmill (Columbus Instruments, Columbus, OH) using a graded maximal exercise test. Briefly, after 3 spaced training sessions for acclimatization, maximal exercise capacity was determined by changing treadmill settings (speed, duration, inclination) until exhaustion as follows: (0 m/min, 3 min, 0°), (6 m/min, 2 min, 0°), (9 m/min, 2 min, 5°), (12 m/min, 2 min, 10°), (15 m/min, 2 min, 15°), (18, 21, 23, 24 m/min, 1 min, 15°), and (+1 m/min, each 1 min thereafter, 15°). The maximum running speed (V_{peak}) is defined as the treadmill speed (in m/min) at which exhaustion is reached.

Invasive Hemodynamic Monitoring

Invasive monitoring of left ventricular diastolic function was conducted with a 2-French Mikro-Tip catheter transducer (Millar, Houston, TX) connected to a PowerLab data acquisition system (ADInstruments, Colorado Springs, CO). In brief, rats were anesthetized with isoflurane and the amount of isoflurane dispensed (1%–2% isoflurane in 100% O₂) was individually adjusted to maintain similar heart rate between animals. A small incision was made through the diaphragm of the rats to insert the tip of the catheter into the LV through the apex of the heart. The left ventricular diastolic time constant, Tau, was calculated with LabChart 8 software (ADInstruments) following the Weiss method.

Real-time Polymerase Chain Reaction

Total RNAs were extracted using RNeasy Fibrous Tissue Kit and their integrity checked on QIAxcel Advanced System (QIAGEN, Germantown, MD). One microgram of total RNA was reverse-transcribed with RevertAid reverse transcriptase using random hexamers as per manufacturer's instructions (Thermo Fisher Scientific, Waltham, MA). TaqMan gene expression assays were used to perform relative quantification of mRNAs encoding atrial natriuretic peptide (Nppa); myosin heavy chain alpha, Myh6; myosin heavy chain beta, Myh7; and sarcoplasmic/

endoplasmic reticulum Ca²⁺ ATPase 2 (SERCA2; Atp2a2) with the standard curve method. Gene expression levels were normalized with quantification of peptidylprolyl isomerase A (Cyclophilin A; Ppia) as the housekeeping gene.

Histology and Immunofluorescence

Formalin-fixed tissue samples were embedded in paraffin, serially cut into 5- μ m-thick sections and processed for Masson Trichrome staining at AML Laboratories (Jacksonville, FL). Separate tissue sections were incubated with fluorescein-labeled wheat germ agglutinin (Vector Laboratories, Burlingame, CA) for 1 hour before staining of cell nuclei with 4',6-diamidino-2-phenylindole. Sections were imaged on a Lionheart FX Automated Microscope and analyzed with Gen5 data collection and analysis software (BioTek Instruments, Winooski, VT).

Transmission Electron Microscopy

Left ventricular tissue samples (≈ 1 mm³) were quickly dissected following euthanasia and immediately fixed in glutaraldehyde. After thin sectioning (70 nm in thickness) and application on copper grids, the stained samples were loaded in a JEM-1400Plus transmission electron microscope (JEOL USA, Peabody, MA) for data acquisition. The entire tissue sections were thoroughly viewed at low magnification ($\times 300$) to ensure integrity and quality of stained tissues before image acquisition. At least five randomly picked fields per sample were examined at higher magnifications.

Western Blotting

Frozen heart tissue samples were homogenized with a Bio-Gen PRO200 Homogenizer (PRO Scientific, Oxford, CT) in protein lysis buffer containing 2.5 mmol/L EGTA, 2.5 mmol/L EDTA, 20 mmol/L KCl, 40 mmol/L beta-glycerophosphate, 40 mmol/L NaF, 4 mmol/L NaPPi, 10% (v/v) glycerol, 0.1% (v/v) Nonidet-P40, cOmplete protease inhibitor cocktail and phosphatase inhibitor cocktails 2 and 3 (MilliporeSigma, Burlington, MA). Tissue homogenates were subsequently centrifuged at 16 000 \times g for 5 minutes at 4 °C and protein concentration of the supernatant determined by bicinchoninic acid assay. Proteins were separated by polyacrylamide gel electrophoresis in reducing sample buffer and transferred to 0.45 μ m pore size polyvinylidene difluoride membranes. Membranes were blocked for 1 hour with 5% (w/v) milk in 1 \times Tris-buffered saline, 0.4% (v/v) Tween 20, at room temperature and incubated overnight at 4 °C with primary antibodies diluted in blocking solution. Antibodies used to detect cardiac troponin I (cTnI; #13083), cTnI phosphorylation at Ser23/24 (#4004), vasodilator-stimulated phosphoprotein phosphorylation at Ser239 (#3114) and HSP 60 (heat shock protein 60; #12165) were from Cell

Signaling Technology (Danvers, MA). Antibodies recognizing UCP3 (ab193470), cTnI phosphorylation at Ser150 (ab169867) and 4-hydroxynonenal-protein adducts (ab46545) were from Abcam (Cambridge, MA). The anti-cysteine sulfenic acid antibody was purchased from MilliporeSigma (Catalog No. 07-2139). Protein detection was performed on the following day using horseradish peroxidase-conjugated anti-rabbit or anti-mouse secondary antibodies and chemiluminescent substrate (Thermo Fisher Scientific). Densitometry band quantifications were performed with ImageJ version 1.53g (National Institutes of Health, Bethesda, MD).

Statistical Analysis

Data are expressed as mean \pm SEM. GraphPad Prism Software (ver 9.0; La Jolla, CA) was used for the statistical analysis. Blood pressure and heart rate were statistically analyzed with use of a 2-way repeated measures ANOVA followed by the Tukey test using time and treatment group as the main factors, and with inclusion of the interaction between these 2 factors. All other multiple comparisons were performed with use of a 2-way ANOVA followed by the Tukey test using genotype and treatment as the main factors. Pairwise comparisons were performed using a 2-tailed paired t-test. $P < 0.05$ was considered significant.

RESULTS

Blood Pressure Response to HS/Ang II Treatment Is Not Affected by UCP3 Insufficiency

Non-invasive tail-cuff measurements demonstrated that mean arterial pressure of 10-week-old male *ucp3^{+/-}* rats maintained on a low-salt diet (124 \pm 3 mm Hg; $n=15$) was comparable with that of the *ucp3^{+/+}* controls (121 \pm 4 mm Hg; $n=9$), and the values remained unaffected by 4 weeks of saline infusion. While high dietary salt intake alone didn't have any impact on blood pressure either, mean arterial pressure started to increase similarly in both genotypes after beginning of Ang II infusion (Figure 2A). Blood pressure rose sharply by an average of 29 mm Hg ($P < 0.01$) at the end of the first week of HS/Ang II treatment before reaching a plateau at the end of the second week. At the end of the fourth week of treatment, blood pressure in the *ucp3^{+/-}* rats (158 \pm 4 mm Hg) was still comparable with that of the *ucp3^{+/+}* rats (155 \pm 7 mm Hg; Figure 2B). Heart rate was stable over time and remained unaffected by treatments until end of the experiment (Figure 2C). Aortic root size increased to the same extent in *ucp3^{+/+}* and *ucp3^{+/-}* rats at completion of the HS/Ang II treatment (Figure 2D). As expected, UCP3 levels were decreased

by $\approx 50\%$ in hearts of *ucp3^{+/-}* rats. Interestingly, HS/Ang II treatment further decreased cardiac UCP3 levels in *ucp3^{+/-}* rats (Figure 2E).

UCP3 Insufficiency Increases LV Wall Thickness in Hypertensive Rats

The decrease in UCP3 levels had no impact on the body weight of adult rats maintained on low-salt diet and infused with saline (Figure 3A). Rats from both genotypes also maintained normal body weight when subjected to HS/Ang II but experienced a similar increase in total heart weight (Figures 3B and 3C). While transthoracic echocardiography confirmed the comparable increase in LV mass on HS/Ang II the analysis revealed greater thickening of the LV anterior and posterior walls and a trend toward greater reduction in LV internal diameter ($P=0.06$) for the *ucp3^{+/-}* rats when compared with their respective non-treated controls (). This observation was supported at the cellular level by a greater increase in myocyte width (+24% for *ucp3^{+/-}* versus +10% for *ucp3^{+/+}*; $P < 0.01$). Conversely, the length of ventricular myocytes was not further affected by UCP3 insufficiency (Figure 3D).

UCP3 Insufficiency Exacerbates Development of LVDD Associated With HS/Ang II-Induced Hypertension

In consistency with our previous study,¹⁰ all baseline LV functional parameters were normal for *ucp3^{+/-}* rats (Table). While indices of systolic function remained unaffected over the whole duration of the experimental protocol, the diastolic function parameters describing LV filling pressure (E/e') and LV relaxation (isovolumic relaxation time) increased after 2 weeks of HS/Ang II treatment for the *ucp3^{+/+}* rats. This increase was maintained until the end of the protocol and coincided with impairment of global LV function as determined by increased myocardial performance index. The *ucp3^{+/-}* rats experienced a similar rise in E/e' , isovolumic relaxation time, and myocardial performance index values after 2 weeks on HS/Ang II. However, those indices continued to deteriorate to become more elevated than that of the *ucp3^{+/+}* rats at completion of the protocol (Figure 4). Invasive monitoring of LV pressure also revealed a greater increase in Tau for *ucp3^{+/-}* rats subjected to HS/Ang II (Table and Figure 4E).

UCP3 Insufficiency Promotes Exercise Intolerance in Hypertensive Rats

Decreased diastolic function is the strongest echocardiographic predictor of impaired exercise tolerance.¹⁸ Baseline exercise capacity was similar

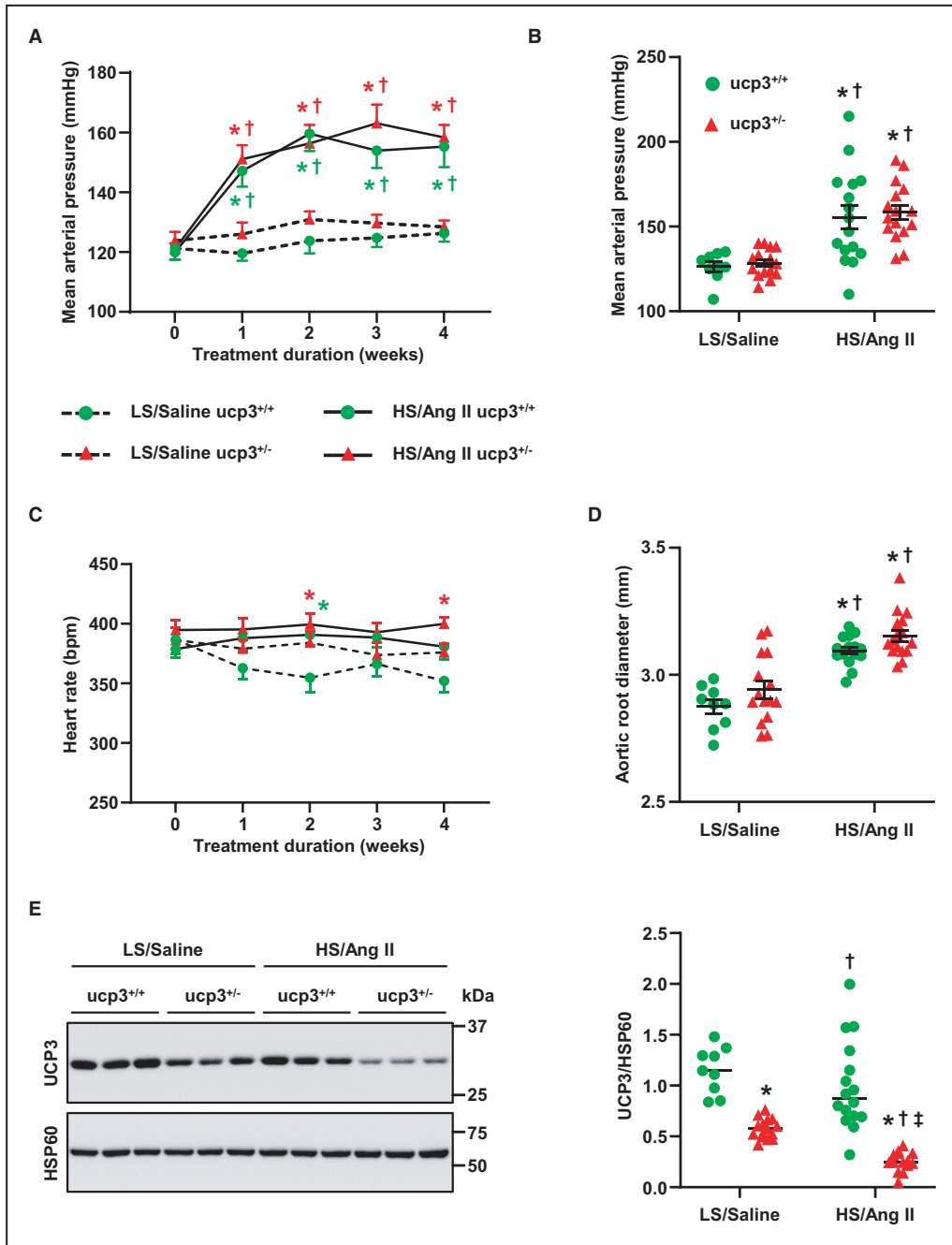


Figure 2. Increased mean arterial pressure in response to high dietary salt intake and Ang II infusion.

A, Weekly mean arterial pressure value of *ucp3*^{-/-} and *ucp3*^{+/+} rats subjected to a combination of high dietary salt intake and Ang II infusion for 4 weeks (HS/Ang II; solid lines). Control animals were fed a low-salt diet and infused with saline (LS/Saline; dashed lines). **B**, Individual blood pressure values at end of treatments. **C**, Weekly heart rate values. **D**, Aortic root diameter values and **(E)** UCP3 levels in the LV at the end of the study protocol. Protein amounts were normalized to heat shock protein 60 (HSP60) levels. Data are expressed as mean±SEM. Data were analyzed by 2-way repeated measures ANOVA (**A** and **C**) or 2-way ANOVA (**B**, **D**, and **E**) with Tukey test. HS/Ang II indicates high dietary salt intake and Ang II infusion; LS/Saline, low-salt diet and infused with saline; and UCP3, uncoupling protein 3. *P*<0.05 vs [†]LS/Saline *ucp3*^{+/+}, [‡]LS/Saline *ucp3*^{-/-}, and [§]HS/Ang II *ucp3*^{+/+}.

between all 4 experimental groups. In addition, exercise capacity remained unchanged at the end of the experimental protocol for animals in the

control groups and for HS/Ang II-treated *ucp3*^{+/+} rats. Conversely, *ucp3*^{-/-} rats on HS/Ang II experienced a decrease in maximum running speed from

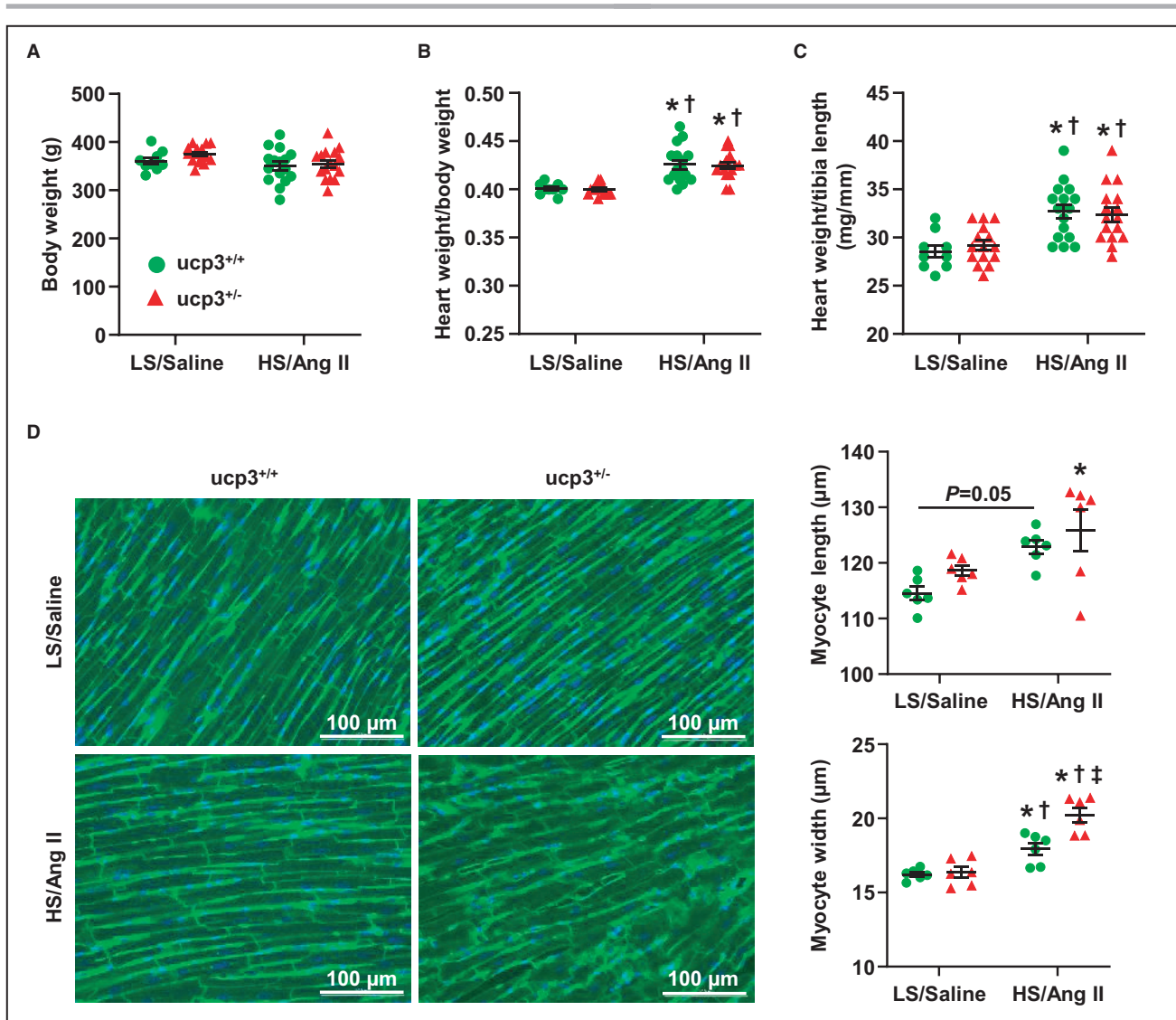


Figure 3. Exacerbation of cardiomyocytes hypertrophy in the left ventricle of *ucp3*^{+/-} rats during hypertension.

A, Body weight, **(B)** heart-to-body weight ratio, and **(C)** heart weight to tibia length ratio in rats after 4 weeks of a combination treatment with high dietary salt intake and Ang II infusion (HS/Ang II) and control animals fed a low-salt diet and infused with saline (LS/Saline). **D**, Cell membranes and nuclei were visualized in the LV at end of treatment with wheat germ agglutinin and 4',6-diamidino-2-phenylindole staining, respectively, and the captured images used to determine cardiomyocytes length and width. A total of 50 cardiomyocytes taken over 5 different fields were measured per animal. Data are expressed as mean±SEM. Data were analyzed by 2-way ANOVA with Tukey test. HS/Ang II indicates high dietary salt intake and Ang II infusion; LS/Saline, low-salt diet and infused with saline; and UCP3, uncoupling protein 3. $P < 0.05$ vs †LS/Saline *ucp3*^{+/-}, ‡LS/Saline *ucp3*^{+/-}, and †HS/Ang II *ucp3*^{+/-}.

baseline values and became exhausted more rapidly (Figures 5A and 5B).

UCP3 Insufficiency Promotes Detrimental Cardiac Remodeling in Response to Hypertension

There was a greater increase in collagen deposition in hearts from HS/Ang II-treated *ucp3*^{+/-} rats when compared with control animals from both genotypes (+170%) or the HS/Ang II-treated *ucp3*^{+/+}

rats (+40%; Figure 6A). In addition, a closer examination of the coronary microvasculature pointed to greater expansion of the perivascular interstitium that was for the most part filled with ground substance (Figure 6B).

Common markers of the fetal gene program include an increase in natriuretic peptides expression, a decrease in sarcoendoplasmic reticulum calcium transport ATPase isoform 2 (SERCA2) mRNA, and myosin heavy chain switching from α to β isoform. All those markers were identified by real-time PCR in the hearts

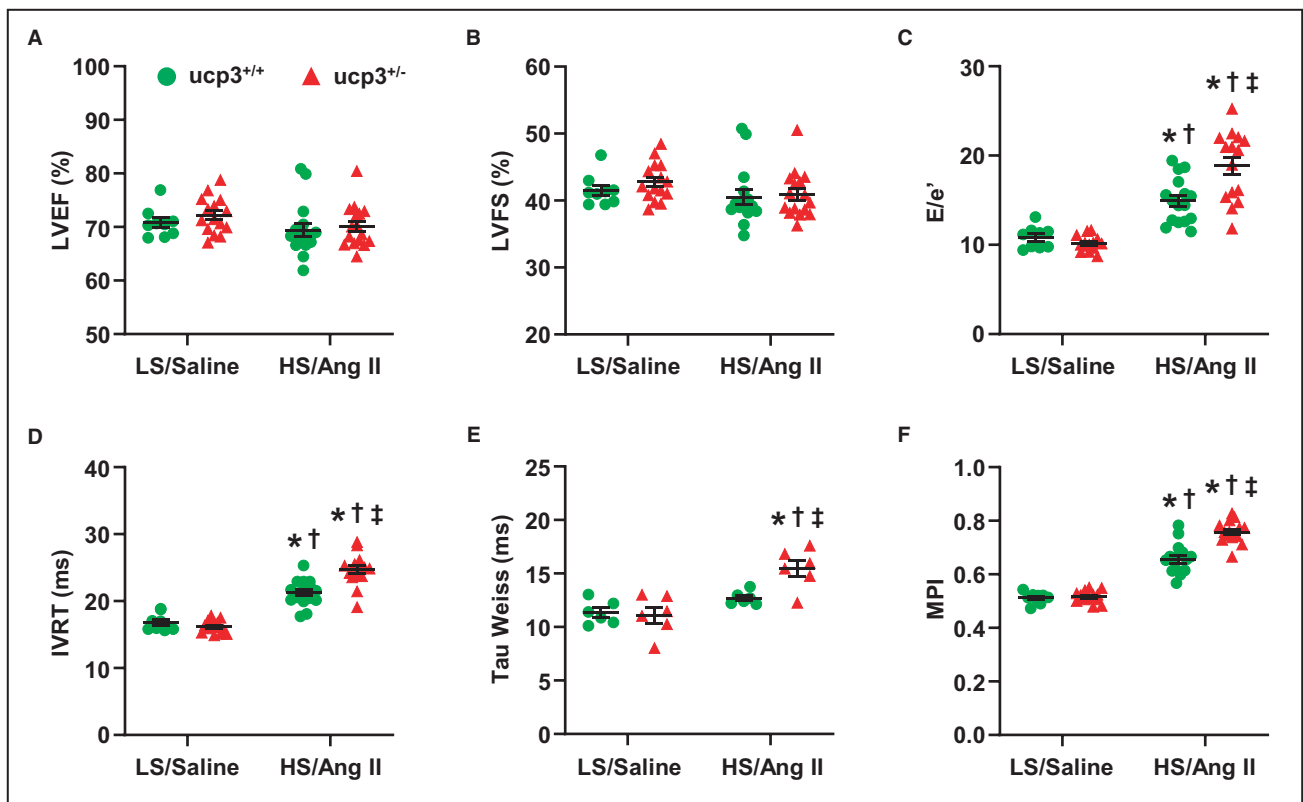


Figure 4. UCP3 (uncoupling protein 3) insufficiency amplifies left ventricular diastolic dysfunction associated with hypertension.

Cardiac functional parameters including left ventricular ejection fraction (A), left ventricular fractional shortening (B), the ratio of E velocity to early diastolic mitral annulus velocity (E/e') (C), the isovolumic relaxation time (D), the diastolic time constant (Tau Weiss) (E), and the myocardial performance index (F) were determined in rats after 4 weeks of a combination treatment with high dietary salt intake and Ang II infusion and in control animals fed a low-salt diet and infused with saline. Data are expressed as mean \pm SEM. Data were analyzed by 2-way ANOVA with Tukey test. E/e' indicates ratio of E velocity to early diastolic mitral annulus velocity; HS/Ang II, high dietary salt intake and Ang II infusion; IVRT, isovolumic relaxation time; LS/Saline, low-salt diet and infused with saline; LVEF, left ventricular ejection fraction; LVFS, left ventricular fractional shortening; and MPI, myocardial performance index. $P < 0.05$ vs LS/Saline ucp3^{+/+}, \dagger LS/Saline ucp3^{+/-}, and \ddagger HS/Ang II ucp3^{+/-}.

of ucp3^{+/-} rats subjected to hypertension (Figure 7A through 7E).

UCP3 Insufficiency Amplifies the Oxidative Stress and Impairment of Protein Kinase G Signaling Associated With Hypertension

4-hydroxynonenal-mediated protein modification is a ROS-induced toxic process occurring when lipid peroxides react with amino acid side chains.¹⁹ Interestingly, while hypertension increased hydroxynonenal-mediated modification of a ≈ 20 kDa protein to a similar level in all animals, the ucp3^{+/-} genotype specifically led to hydroxynonenal-mediated modification of another protein with a molecular weight exceeding 250 kDa (Figure 8A). Cysteine sulfenation of proteins also increased 2-fold in hearts of hypertensive ucp3^{+/-} rats (Figure 8B). Oxidative stress predisposes to low myocardial protein kinase G (PKG) activity.²⁰ Accordingly, higher oxidative

stress in hearts of the hypertensive ucp3^{+/-} rats was accompanied by decreased phosphorylation of the PKG target site Ser23/24 on cardiac troponin I (cTnI), a post-translational modification that has been linked to impaired relaxation of cardiomyocytes.²¹ Conversely, the phosphorylation of cTnI at Ser150 which is independent from PKG signaling was not affected by UCP3 insufficiency nor the presence of hypertension (Figure 8C). Because Ser23/24 can also be phosphorylated by protein kinase A,²¹ PKG-specific phosphorylation of vasodilator-stimulated phosphoprotein on Ser239 was also quantified and found to be decreased specifically in hearts of HS/Ang II-treated ucp3^{+/-} rats (Figure 8D).

DISCUSSION

Impaired ventricular diastolic function is exceedingly common in hypertensive patients with obesity and diabetes,^{5,6} yet the reasons for this negative synergy

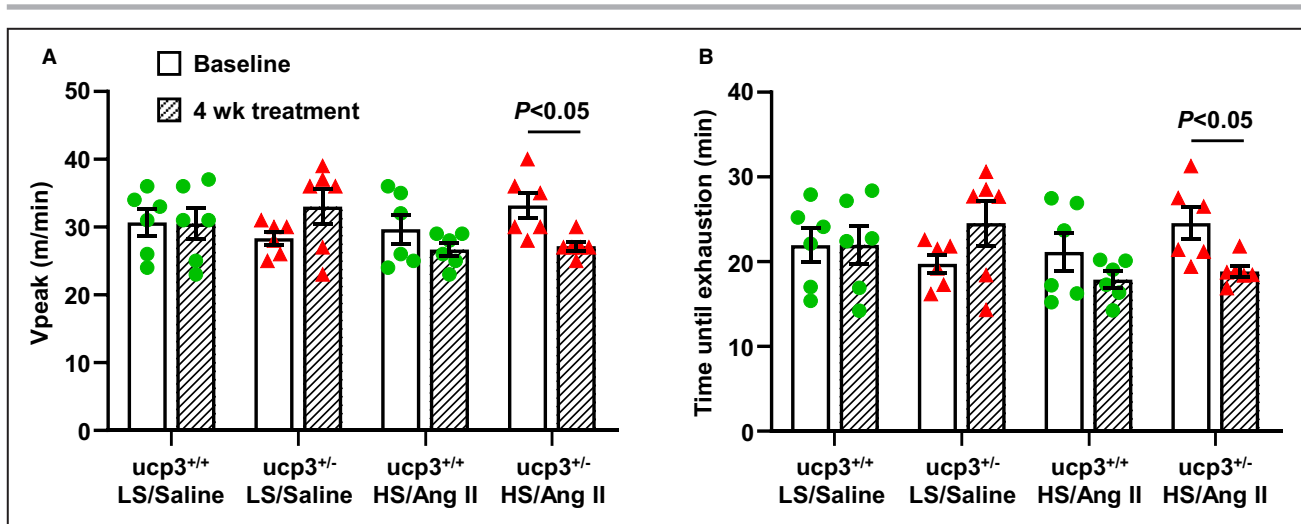


Figure 5. Decreased tolerance to exercise for *ucp3*^{+/-} rats during hypertension.

A, The maximum running speed on a treadmill (*V*_{peak}) and **(B)** time until exhaustion was reached were determined for *ucp3*^{+/-} and *ucp3*^{+/+} rats before (baseline) and after 4 weeks of a combination treatment with high dietary salt intake and Ang II infusion (HS/Ang II). Control animals were fed a low-salt diet and infused with 0.9% saline. Data are expressed as mean±SEM. Data were analyzed with 2-tailed paired t-test. HS/Ang II indicates high dietary salt intake and Ang II infusion; LS/Saline, low-salt diet and infused with saline; and UCP3, uncoupling protein 3. *P*<0.05 was considered significant.

remain incompletely understood. In the present study we demonstrate that a partial loss in UCP3, such as has been observed with obesity and type 2 diabetes, is sufficient to exacerbate per se the development of LVDD and exercise intolerance during hypertension. Mechanistically, UCP3 insufficiency led to the amplification of detrimental remodeling events that have been linked to increased myocardial stiffness and impaired LV relaxation. Those events included excess LV wall thickening, alterations in the composition and expansion of the extracellular matrix (ECM), reactivation of the fetal gene program and impairment of PKG signaling. Based on our previously published data and work from others,⁸⁻¹⁰ we propose increased oxidative stress as the root cause for exacerbation of this adverse myocardial remodeling.

Intrinsic LV abnormalities such as LV hypertrophy play a key role in the development of diastolic dysfunction. It is well established that increased LV wall thickness is an independent predictor of diastolic stiffness.²² Hence, a worsening of LV concentric hypertrophy caused by a greater enlargement of cardiomyocytes may be part of the mechanism by which UCP3 insufficiency precipitates the impairment of diastolic function in our experimental model. While complete loss of UCP3 has previously been suggested to stimulate cardiac hypertrophy through aggravation of high-salt induced hypertension in mice,²³ UCP3 insufficiency was not associated with increased blood pressure response to HS/Ang II. Although we cannot rule out potential changes in the effects of sodium and

Ang II on cardiomyocytes, it is more likely that UCP3 insufficiency exerted an additive pro-hypertrophic effect through increased ROS generation. Indeed, ROS-mediated stimulation of cardiomyocytes growth may occur through inhibition of cGMP-PKG signaling and through activation of the extracellular-signal regulated kinases 1 and 2 (ERK1/2).^{24,25} Even though the modulation of ERK1/2 signaling was not investigated here, our results clearly demonstrate that UCP3 insufficiency contributed to impaired PKG activity in the pressure-overloaded heart.

Changes in the myocardial ECM network, including an increase in interstitial and perivascular fibrosis and an expansion of the interstitial proteoglycan pool, are other well-described causative factors in the impairment of LV compliance and diastolic dysfunction associated with pressure overload, and those detrimental alterations were clearly accelerated with UCP3 insufficiency.²⁶ Because excess ROS generation has been implicated in the activation of a fibrotic response in the diseased and aging hearts,^{26,27} it is plausible that increased oxidative stress induced by lack of UCP3 acted as a central mediator for accelerated remodeling of the ECM in the pressure-overloaded heart. In addition to the exacerbated ECM remodeling, our gene expression analyses also revealed enhanced reactivation of the fetal gene program. Although return to the fetal gene program may initially help the adult heart adapt to a variety of stress conditions, its long-term activation is detrimental to contractility, calcium handling and myocardial energetics and eventually contribute

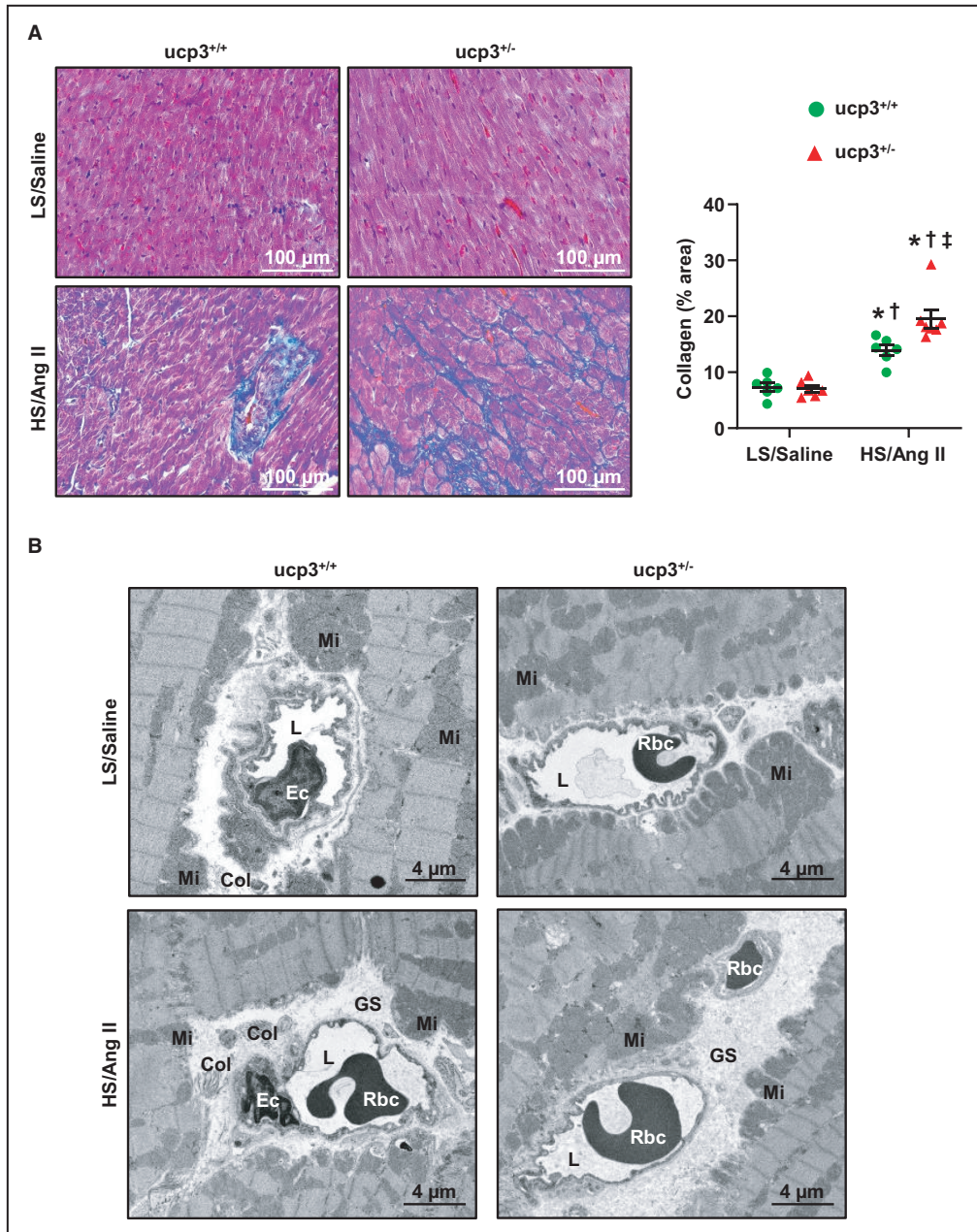


Figure 6. Exacerbation of adverse remodeling in the left ventricle of *ucp3*^{+/-} rats during hypertension.

A, Collagen quantification was performed on whole transverse cardiac sections stained with Masson's Trichrome. Representative photomicrographs are shown. **B**, Visualization of the extracellular matrix around capillaries in the LV of rats at end of treatment. Representative photomicrographs are shown. Data are expressed as mean±SEM. Data were analyzed by 2-way ANOVA with Tukey test. Col indicates collagen; Ec, endothelial cell; GS, ground substance; HS/Ang II, high dietary salt intake and Ang II infusion; L, lumen; LS/Saline, low-salt diet and infused with saline; Mi, mitochondria; Rbc, red blood cell; and UCP3, uncoupling protein 3. $P < 0.05$ vs [†]LS/Saline *ucp3*^{+/+}, [†]LS/Saline *ucp3*^{+/-}, and [‡]HS/Ang II *ucp3*^{+/-}.

to heart failure.²⁸ Thus while the transition from α - to β -myosin heavy chain beta is energetically advantageous, the shift lowers contribution of the atrial contraction to filling of the ventricle, which compromises diastolic function at higher heart rates.²⁹ Decreased expression and activity of the SERCA pump could also

lead to slowed rate of Ca^{2+} reuptake by the sarcoplasmic reticulum and prolongation of muscle relaxation.³⁰ Moreover, elevated plasma atrial natriuretic peptide levels have been associated with early LVDD in patients with diabetes.³¹ This transcriptional remodeling has been associated with increased myocardial

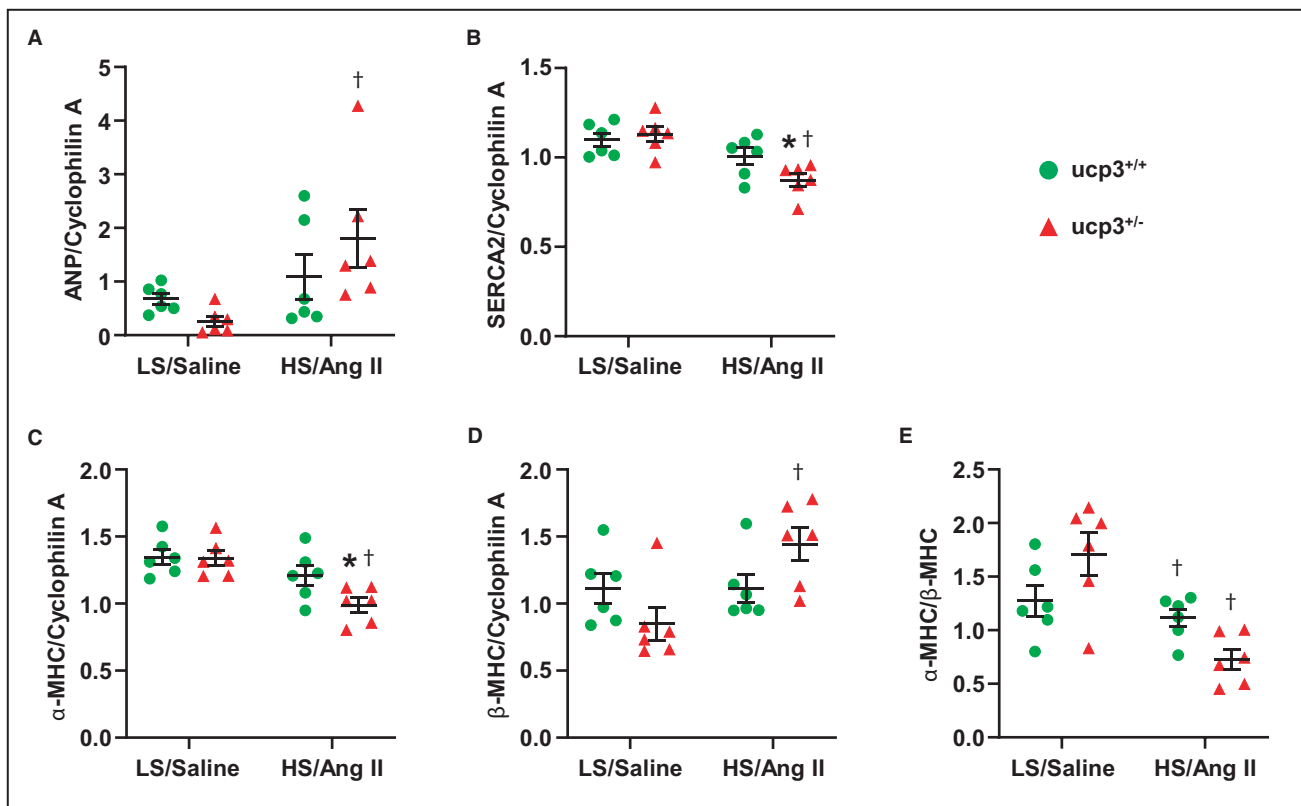


Figure 7. Increased return to the fetal gene program in the left ventricle of *ucp3*^{+/-} rats during hypertension.

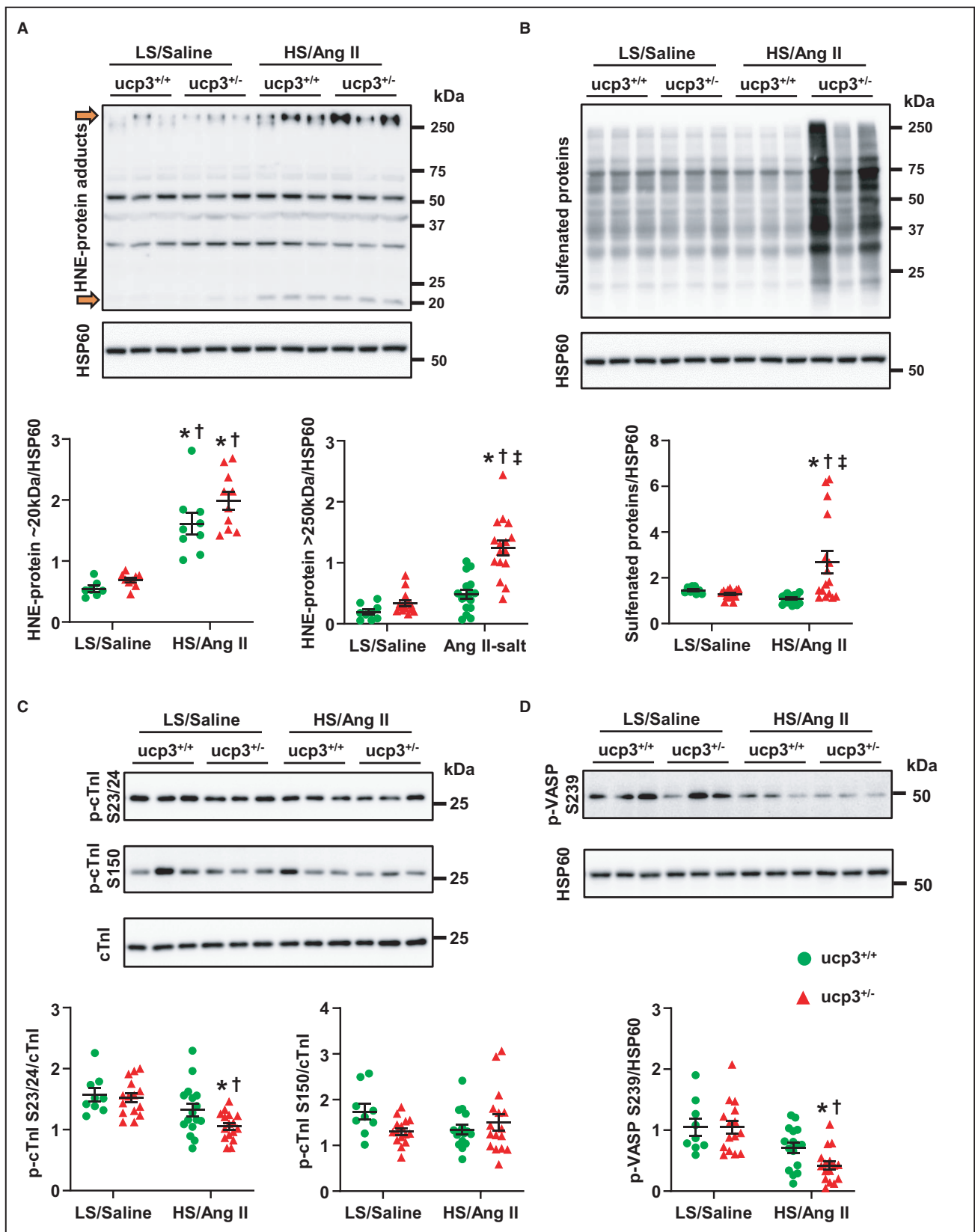
Quantitative changes in the expression of the individual markers (A) atrial natriuretic peptide, (B) sarcoplasmic/endoplasmic reticulum Ca²⁺ ATPase 2 (SERCA2), (C) myosin heavy chain alpha, (D) myosin heavy chain beta, and (E) the myosin heavy chain alpha-to-myosin heavy chain beta, ratio were determined for all groups of animals by real-time polymerase chain reaction. Data are expressed as mean±SEM. Data were analyzed by 2-way ANOVA with Tukey test. α-MHC indicates myosin heavy chain alpha; β-MHC, myosin heavy chain beta; ANP, atrial natriuretic peptide; HS/Ang II, high dietary salt intake and Ang II infusion; LS/Saline, low-salt diet and infused with saline; and UCP3, uncoupling protein 3. *P*<0.05 vs †LS/Saline *ucp3*^{+/+}, and * †LS/Saline *ucp3*^{+/-}.

oxidative stress, and although causality is not clearly established it is noteworthy that deletion of nuclear factor erythroid 2-related factor 2, a master regulator of the endogenous antioxidant defense system, is sufficient to exacerbate return to the fetal gene program in hearts of mice subjected to pressure overload by constriction of the transverse aorta.^{32,33} Therefore, accelerated return to the fetal gene program in hypertensive *ucp3*^{+/-} rats may also be rooted in the excessive ROS generation caused by partial loss of the mitochondrial anion carrier.

Lastly, ROS can affect cardiomyocyte relaxation through direct and indirect modification of certain amino acids, thereby resulting in loss of protein functions and interruption of normal regulatory signals.³⁴ Thus, an increase in protein-bound carbonyls driven by the generation of lipid peroxides and subsequent formation of lipid-protein adducts has been linked to the modification of at least 167 proteins from the cytoskeleton, ECM, cell adhesion and junction components, and ion channels, including several regulators of cellular Ca²⁺ homeostasis.³⁵ The mutual

interplay between Ca²⁺ and ROS signaling systems and its contribution to impairment of myocardial relaxation is particularly well described.³⁶ For example, irreversible oxidative sulfonation of Cys674 in SERCA has been associated with decreased activity of the protein in senescence- and diabetes-related conditions.^{37,38} Another protein well known to be affected by high oxidative stress in the myocardium is PKG, and decreased phosphorylation of PKG targets located in the sarcoplasmic reticulum (phospholamban) and sarcomeres (titin, cTnI) has been consistently associated with impaired diastolic calcium reuptake, increased myocytes stiffening and decreased cell relaxation rate.²⁰ Therefore, by showing that the LV of *ucp3*^{+/-} rats exhibited greater ROS-mediated modification of certain proteins as well as an impairment of PKG-mediated regulation of cardiac contractile components, our results unambiguously support a role for UCP3 insufficiency in the pathogenesis of LVDD during hypertension.

Because our experimental protocol was limited to the study of male rats, whether UCP3 insufficiency



differentially impacts myocardial remodeling during hypertension in females still remains to be investigated. Mounting clinical evidence suggests that a more

pronounced diastolic dysfunction contributes to the greater incidence of HFpEF in women compared with men.^{39,40} While premenopausal women appear to be

Figure 8. Exacerbation of oxidative stress and downregulation of protein kinase G signaling in the left ventricle of *ucp3*^{+/-} rats during hypertension.

A, Quantification of 4-hydroxynonenal protein adducts, **(B)** total protein sulfenation amounts, **(C)** phosphorylation levels of cardiac troponin I at Ser23/24 and Ser150, and **(D)** phosphorylation levels of vasodilator-stimulated phosphoprotein at Ser239 in the left ventricle of *ucp3*^{+/-} and *ucp3*^{+/+} rats after 4 weeks of a combination treatment with high dietary salt intake and Ang II infusion. Control animals were fed a low-salt diet and infused with saline. Protein amounts were normalized to HSP60 (heat shock protein 60) or cardiac troponin I protein levels. Data are expressed as mean±SEM. Data were analyzed by 2-way ANOVA with Tukey test. cTnI indicates cardiac troponin I; HS/Ang II, high dietary salt intake and Ang II infusion; HSP60, heat shock protein 60; LS/Saline, low-salt diet and infused with saline; p-cTnI, phospho-cardiac troponin I; p-VASP, phospho-vasodilator-stimulated phosphoprotein; and UCP3, uncoupling protein 3. *P*<0.05 vs [†]LS/Saline *ucp3*^{+/+}, [‡]LS/Saline *ucp3*^{+/-}, and [‡]HS/Ang II *ucp3*^{+/-}.

less susceptible to oxidative stress,^{41,42} and although LV contractile recovery following myocardial ischemia/reperfusion was similarly impaired in hearts from male

and female *ucp3*^{+/-} rats,¹⁰ a role for UCP3 in the sex difference in diastolic function during hypertension cannot be ruled out at this time.

Table. Transthoracic Echocardiography and Hemodynamic Parameters

Day	Parameter	LS/Saline		HS/Ang II	
		<i>ucp3</i> ^{+/+}	<i>ucp3</i> ^{+/-}	<i>ucp3</i> ^{+/+}	<i>ucp3</i> ^{+/-}
0	HR, bpm	393±12	395±9	384±7	372±6
	LV mass, mg	641±25	732±18	669±22	667±16
	LVAWd, mm	1.47±0.04	1.48±0.04	1.44±0.05	1.49±0.04
	LVIDd, mm	7.52±0.22	8.02±0.14	7.90±0.17	7.78±0.19
	LVPWd, mm	1.60±0.05	1.64±0.04	1.54±0.04	1.51±0.04
	LVEF (%)	73.6±1.2	72.9±0.8	71.5±0.8	72.5±0.5
	LVFS (%)	44.0±1.1	43.6±0.8	42.3±0.7	43.1±0.4
	E/e'	10.7±0.4	10.5±0.3	10.7±0.2	11.1±0.5
	IVRT, ms	15.2±0.4	14.7±0.4	16.4±0.5	16.0±0.5
MPI	0.47±0.01	0.47±0.01	0.49±0.01	0.48±0.01	
14	HR, bpm	387±10	387±4	372±6	373±7
	LV mass, mg	736±16	772±13	788±20	839±33 [*]
	LVAWd, mm	1.51±0.06	1.65±0.05	1.73±0.03 [*]	1.92±0.06 ^{†‡}
	LVIDd, mm	7.80±0.19	7.86±0.11	7.61±0.14	7.41±0.11
	LVPWd, mm	1.74±0.05	1.68±0.05	1.77±0.05	1.85±0.05
	LVEF (%)	71.6±0.7	72.4±0.8	70.9±1.2	71.1±0.5
	LVFS (%)	42.3±0.5	43.1±0.7	41.8±1.0	41.7±0.4
	E/e'	11.2±0.2	10.0±0.2	14.7±0.6 ^{†‡}	14.8±0.8 [†]
	IVRT, ms	16.0±0.3	15.6±0.2	19.4±0.4 [†]	20.4±0.6 [†]
MPI	0.49±0.01	0.49±0.01	0.58±0.01 [†]	0.61±0.01 ^{†‡}	
28	HR, bpm	382±12	380±7	375±5	369±6
	LV mass, mg	797±20	845±22	925±26 [*]	964±33 [†]
	LVAWd, mm	1.74±0.06	1.83±0.06	2.01±0.08	2.21±0.06 [†]
	LVIDd, mm	7.49±0.16	7.69±0.14	7.42±0.19	7.15±0.12
	LVPWd, mm	1.87±0.06	1.81±0.06	2.04±0.06 [†]	2.10±0.06 [†]
	LVEF (%)	70.8±0.9	72.2±0.9	69.5±1.2	70.1±1.0
	LVFS (%)	41.5±0.8	42.8±0.7	40.5±1.1	40.9±0.9
	E/e'	10.8±0.4	10.2±0.2	14.9±0.6 [†]	18.8±1.0 ^{†‡}
	IVRT, ms	16.8±0.4	16.2±0.2	21.3±0.5 ^{†‡}	24.7±0.6 ^{†‡}
	MPI	0.51±0.01	0.52±0.01	0.66±0.01 [†]	0.76±0.01 ^{†‡}
	Tau Weiss, ms	11.3±0.4	11.1±0.7	12.7±0.2	15.5±0.8 ^{†‡}

E/e' indicates ratio of E velocity to early diastolic mitral annulus velocity; HR, heart rate; HS/Ang II, high dietary salt intake and Ang II infusion; IVRT, isovolumic relaxation time; LV, left ventricular; LS/Saline, low-salt diet and infused with saline; LVAWd, left ventricular anterior wall thickness at end-diastole; LVEF, left ventricular ejection fraction; LVFS, left ventricular fractional shortening; LVIDd, left ventricular internal diameter at end-diastole; LVPWd, left ventricular posterior wall thickness at end-diastole; MPI, myocardial performance index; and *ucp3*, uncoupling protein 3. Data were analyzed by 2-way ANOVA with Tukey test. *P*<0.05 vs [†]LS/Saline *ucp3*^{+/+}, [‡]LS/Saline *ucp3*^{+/-}, and [‡]HS/Ang II *ucp3*^{+/-}. n=9–16 for all parameters except for Tau Weiss (n=6).

CONCLUSIONS

Our findings shed light on mitochondrial oxidative stress mediated by UCP3 insufficiency as a cause for increased incidence of LVDD and exercise intolerance during hypertension. Considering previously published observations that UCP3 insufficiency is a pathological feature of myocytes in obesity, insulin resistance, and type 2 diabetes,^{10,14,15} the new findings provide an explanation as to how those metabolic disorders synergize with high blood pressure to precipitate development of LVDD and progression toward HFpEF. In addition, our results add further support to the use of antioxidants targeting mitochondrial ROS as an adjuvant therapy to antihypertensives for preventing HFpEF progression in individuals with obesity. Although we acknowledge that clinically improving heart failure symptoms with vitamins C or E has yielded mixed results, the lack of specificity of those antioxidants for mitochondrial ROS and their use at a late stage of the disease could be the reason for their inefficacy.¹¹ Conversely, there is strong preclinical evidence that boosting mitochondrial antioxidant defenses provides additional therapeutic benefits by decreasing cardiac inflammation, improving LVDD, and even lowering blood pressure.^{43,44} Future studies will aim to determine the efficacy of such treatment regimens in animal models of hypertension associated with UCP3 insufficiency and obesity.

ARTICLE INFORMATION

Received June 4, 2021; accepted July 30, 2021.

Affiliations

Department of Physiology and Biophysics (X.C., S.A., R.H.) and Mississippi Center for Obesity Research (X.C., S.A., R.H.), University of Mississippi Medical Center, Jackson, MS; and Jinnah Hospital, Lahore, Punjab, Pakistan (N.A.).

Acknowledgments

The authors thank Glenn A. Hoskins (University of Mississippi Medical Center) for his assistance with the preparation and analysis of transmission electron microscopy samples.

Sources of Funding

This work was supported by grants R01HL136438, P20GM104357, and P01HL051971 from the National Institutes of Health. The content of the article is solely the responsibility of the authors and does not necessarily represent the official views of the National Institutes of Health.

Disclosures

None.

REFERENCES

- Shah KS, Xu H, Matsouaka RA, Bhatt DL, Heidenreich PA, Hernandez AF, Devore AD, Yancy CW, Fonarow GC. Heart failure with preserved, borderline, and reduced ejection fraction: 5-year outcomes. *J Am Coll Cardiol*. 2017;70:2476–2486. doi: 10.1016/j.jacc.2017.08.074
- Wan SH, Vogel MW, Chen HH. Pre-clinical diastolic dysfunction. *J Am Coll Cardiol*. 2014;63:407–416. doi: 10.1016/j.jacc.2013.10.063
- Poirier P, Bogaty P, Garneau C, Marois L, Dumesnil JG. Diastolic dysfunction in normotensive men with well-controlled type 2 diabetes: importance of maneuvers in echocardiographic screening for preclinical diabetic cardiomyopathy. *Diabetes Care*. 2001;24:5–10. doi: 10.2337/diacare.24.1.5
- Russo C, Jin Z, Homma S, Rundek T, Elkind MS, Sacco RL, Di Tullio MR. Effect of obesity and overweight on left ventricular diastolic function: a community-based study in an elderly cohort. *J Am Coll Cardiol*. 2011;57:1368–1374. doi: 10.1016/j.jacc.2010.10.042
- Kim J, Kim MG, Kang S, Kim BR, Baek MY, Park YM, Shin MS. Obesity and hypertension in association with diastolic dysfunction could reduce exercise capacity. *Korean Circ J*. 2016;46:394–401. doi: 10.4070/kcj.2016.46.3.394
- Russo C, Jin Z, Homma S, Rundek T, Elkind MS, Sacco RL, Di Tullio MR. Effect of diabetes and hypertension on left ventricular diastolic function in a high-risk population without evidence of heart disease. *Eur J Heart Fail*. 2010;12:454–461. doi: 10.1093/eurjhf/hfq022
- Pohl EE, Rupprecht A, Macher G, Hilse KE. Important trends in UCP3 investigation. *Front Physiol*. 2019;10:470. doi: 10.3389/fphys.2019.00470
- Vidal-Puig AJ, Grujic D, Zhang CY, Hagen T, Boss O, Ido Y, Szczepanik A, Wade J, Mootha V, Cortright R, et al. Energy metabolism in uncoupling protein 3 gene knockout mice. *J Biol Chem*. 2000;275:16258–16266. doi: 10.1074/jbc.M910179199
- Ozcan C, Palmeri M, Horvath TL, Russell KS, Russell RR III. Role of uncoupling protein 3 in ischemia-reperfusion injury, arrhythmias, and preconditioning. *Am J Physiol Heart Circ Physiol*. 2013;304:H1192–1200. doi: 10.1152/ajpheart.00592.2012
- Edwards KS, Ashraf S, Lomax TM, Wiseman JM, Hall ME, Gava FN, Hall JE, Hosler JP, Harmancey R. Uncoupling protein 3 deficiency impairs myocardial fatty acid oxidation and contractile recovery following ischemia/reperfusion. *Basic Res Cardiol*. 2018;113:47. doi: 10.1007/s00395-018-0707-9
- Munzel T, Gori T, Keaney JF Jr, Maack C, Daiber A. Pathophysiological role of oxidative stress in systolic and diastolic heart failure and its therapeutic implications. *Eur Heart J*. 2015;36:2555–2564. doi: 10.1093/eurheartj/ehv305
- Bovo E, Mazurek SR, de Tombe PP, Zima AV. Increased energy demand during adrenergic receptor stimulation contributes to Ca²⁺ wave generation. *Biophys J*. 2015;109:1583–1591. doi: 10.1016/j.bpj.2015.09.002
- Dai DF, Johnson SC, Villarin JJ, Chin MT, Nieves-Cintrón M, Chen T, Marcinek DJ, Dorn GW II, Kang YJ, Prolla TA, et al. Mitochondrial oxidative stress mediates angiotensin II-induced cardiac hypertrophy and galphaq overexpression-induced heart failure. *Circ Res*. 2011;108:837–846. doi: 10.1161/CIRCRESAHA.110.232306
- Schrauwen P, Mensink M, Schaart G, Moonen-Kornips E, Sels JP, Blaak EE, Russell AP, Hesselink MK. Reduced skeletal muscle uncoupling protein-3 content in prediabetic subjects and type 2 diabetic patients: restoration by rosiglitazone treatment. *J Clin Endocrinol Metab*. 2006;91:1520–1525. doi: 10.1210/jc.2005-1572
- Boudina S, Han YH, Pei S, Tidwell TJ, Henrie B, Tuinei J, Olsen C, Sena S, Abel ED. UCP3 regulates cardiac efficiency and mitochondrial coupling in high fat-fed mice but not in leptin-deficient mice. *Diabetes*. 2012;61:3260–3269. doi: 10.2337/db12-0063
- Osborn JW, Fink GD, Sved AF, Toney GM, Raizada MK. Circulating angiotensin II and dietary salt: converging signals for neurogenic hypertension. *Curr Hypertens Rep*. 2007;9:228–235. doi: 10.1007/s11906-007-0041-3
- Lomax TM, Ashraf S, Yilmaz G, Harmancey R. Loss of uncoupling protein 3 attenuates western diet-induced obesity, systemic inflammation, and insulin resistance in rats. *Obesity (Silver Spring)*. 2020;28:1687–1697. doi: 10.1002/oby.22879
- Grewal J, McCully RB, Kane GC, Lam C, Pellikka PA. Left ventricular function and exercise capacity. *JAMA*. 2009;301:286–294. doi: 10.1001/jama.2008.1022
- Castro JP, Jung T, Grune T, Siems W. 4-Hydroxynonenal (HNE) modified proteins in metabolic diseases. *Free Radic Biol Med*. 2017;111:309–315. doi: 10.1016/j.freeradbiomed.2016.10.497
- Kovacs A, Alogna A, Post H, Hamdani N. Is enhancing cGMP-PKG signalling a promising therapeutic target for heart failure with preserved ejection fraction? *Neth Heart J*. 2016;24:268–274. doi: 10.1007/s12471-016-0814-x
- Layland J, Solaro RJ, Shah AM. Regulation of cardiac contractile function by troponin I phosphorylation. *Cardiovasc Res*. 2005;66:12–21. doi: 10.1016/j.cardiores.2004.12.022

22. Grossman W, McLaurin LP, Moos SP, Stefadouros M, Young DT. Wall thickness and diastolic properties of the left ventricle. *Circulation*. 1974;49:129–135. doi: 10.1161/01.CIR.49.1.129
23. Lang H, Xiang Y, Ai Z, You Z, Jin X, Wan Y, Yang Y. UCP3 ablation exacerbates high-salt induced cardiac hypertrophy and cardiac dysfunction. *Cell Physiol Biochem*. 2018;46:1683–1692. doi: 10.1159/000489244
24. Nakamura T, Zhu G, Ranek MJ, Kokkonen-Simon K, Zhang M, Kim GE, Tsujita K, Kass DA. Prevention of PKG-1 α oxidation suppresses antihypertrophic/antifibrotic effects from PDE5 inhibition but not SGC stimulation. *Circ Heart Fail*. 2018;11:e004740. 00740. doi: 10.1161/CIRCHEARTFAILURE.117.004740
25. Tanaka K, Honda M, Takabatake T. Redox regulation of MAPK pathways and cardiac hypertrophy in adult rat cardiac myocyte. *J Am Coll Cardiol*. 2001;37:676–685. doi: 10.1016/S0735-1097(00)01123-2
26. Frangogiannis NG. The extracellular matrix in ischemic and nonischemic heart failure. *Circ Res*. 2019;125:117–146. doi: 10.1161/CIRCRESAHA.119.311148
27. Takimoto E, Kass DA. Role of oxidative stress in cardiac hypertrophy and remodeling. *Hypertension*. 2007;49:241–248. doi: 10.1161/01.HYP.0000254415.31362.a7
28. Dirx E, da Costa Martins PA, De Windt LJ. Regulation of fetal gene expression in heart failure. *Biochim Biophys Acta*. 2013;1832:2414–2424. doi: 10.1016/j.bbadis.2013.07.023
29. Narolska NA, Eiras S, van Loon RB, Boontje NM, Zaremba R, Spiegelenberg SR, Stooker W, Huybregts M, Visser FC, van der Velden J, et al. Myosin heavy chain composition and the economy of contraction in healthy and diseased human myocardium. *J Muscle Res Cell Motil*. 2005;26:39–48. doi: 10.1007/s10974-005-9005-x
30. Periasamy M, Janssen PM. Molecular basis of diastolic dysfunction. *Heart Fail Clin*. 2008;4:13–21. doi: 10.1016/j.hfc.2007.10.007
31. Bayerle-Eder M, Zangeneh M, Kreiner G, Raffesberg W, Nowotny P, Vierhapper H, Waldhausl W, Wolzt M, Pleiner H, Gasic S. ANP but not BNP reflects early left diastolic dysfunction in type 1 diabetics with myocardial dysinnervation. *Horm Metab Res*. 2003;35:301–307. doi: 10.1055/s-2003-41306
32. Li J, Ichikawa T, Villacorta L, Janicki JS, Brower GL, Yamamoto M, Cui T. Nrf2 protects against maladaptive cardiac responses to hemodynamic stress. *Arterioscler Thromb Vasc Biol*. 2009;29:1843–1850. doi: 10.1161/ATVBAHA.109.189480
33. Rosa C, Xavier N, Henrique Campos D, Fernandes AA, Cezar MD, Martinez P, Cicogna A, Gimenes C, Gimenes R, Okoshi M, et al. Diabetes mellitus activates fetal gene program and intensifies cardiac remodeling and oxidative stress in aged spontaneously hypertensive rats. *Cardiovasc Diabetol*. 2013;12:152. doi: 10.1186/1475-2840-12-152
34. Davies MJ. Protein oxidation and peroxidation. *Biochem J*. 2016;473:805–825. doi: 10.1042/BJ20151227
35. Griesser E, Vemula V, Raulien N, Wagner U, Reeg S, Grune T, Fedorova M. Cross-talk between lipid and protein carbonylation in a dynamic cardiomyocyte model of mild nitroxidative stress. *Redox Biol*. 2017;11:438–455. doi: 10.1016/j.redox.2016.12.028
36. Gorlach A, Bertram K, Hudecova S, Krizanova O. Calcium and ROS: a mutual interplay. *Redox Biol*. 2015;6:260–271. doi: 10.1016/j.redox.2015.08.010
37. Qin F, Siwik DA, Lancel S, Zhang J, Kuster GM, Luptak I, Wang L, Tong X, Kang YJ, Cohen RA, et al. Hydrogen peroxide-mediated SERCA cysteine 674 oxidation contributes to impaired cardiac myocyte relaxation in senescent mouse heart. *J Am Heart Assoc*. 2013;2:e000184. doi: 10.1161/JAHA.113.000184
38. Tong X, Ying J, Pimentel DR, Trucillo M, Adachi T, Cohen RA. High glucose oxidizes SERCA cysteine-674 and prevents inhibition by nitric oxide of smooth muscle cell migration. *J Mol Cell Cardiol*. 2008;44:361–369. doi: 10.1016/j.yjmcc.2007.10.022
39. Gori M, Lam CSP, Gupta DK, Santos ABS, Cheng S, Shah AM, Claggett B, Zile MR, Kraigher-Krainer E, Pieske B, et al. Sex-specific cardiovascular structure and function in heart failure with preserved ejection fraction. *Eur J Heart Fail*. 2014;16:535–542. doi: 10.1002/ejhf.67
40. Sotomi Y, Hikoso S, Nakatani D, Mizuno H, Okada K, Dohi T, Kitamura T, Sunaga A, Kida H, Oeun B, et al. Sex differences in heart failure with preserved ejection fraction. *J Am Heart Assoc*. 2021;10:e018574. doi: 10.1161/JAHA.120.018574
41. Kander MC, Cui Y, Liu Z. Gender difference in oxidative stress: a new look at the mechanisms for cardiovascular diseases. *J Cell Mol Med*. 2017;21:1024–1032. doi: 10.1111/jcmm.13038
42. Lagranha CJ, Deschamps A, Aponte A, Steenbergen C, Murphy E. Sex differences in the phosphorylation of mitochondrial proteins result in reduced production of reactive oxygen species and cardioprotection in females. *Circ Res*. 2010;106:1681–1691. doi: 10.1161/CIRCRESAHA.109.213645
43. Cieslik KA, Sekhar RV, Granillo A, Reddy A, Medrano G, Heredia CP, Entman ML, Hamilton DJ, Li S, Reineke E, et al. Improved cardiovascular function in old mice after N-acetyl cysteine and glycine supplemented diet: inflammation and mitochondrial factors. *J Gerontol A Biol Sci Med Sci*. 2018;73:1167–1177. doi: 10.1093/gerona/gly034
44. Dikalova AE, Bikineyeva AT, Budzyn K, Nazarewicz RR, McCann L, Lewis W, Harrison DG, Dikalov SI. Therapeutic targeting of mitochondrial superoxide in hypertension. *Circ Res*. 2010;107:106–116. doi: 10.1161/CIRCRESAHA.109.214601